# Addressing single spin crossover molecules in a two-dimensional monolayer

**Yongfeng Tong**
SOLEIL-Synchrotron
**Massine Kelaï**
Université de Paris / CNRS
**Kaushik Bairagi**
Université de Paris / CNRS
**Vincent Repain**
Université de Paris / CNRS
**Jérôme Lagoute**
Université de Paris / CNRS
**Yann Girard**
Université de Paris / CNRS
**Sylvie Rousset**
Université de Paris / CNRS
**Marie-Laure Boillot**
Université Paris-Saclay / CNRS
**Talal Mallah**
Université Paris-Sud 11
**Cristian Enachescu**
Alexandru Ioan Cuza University of Iasi
**Amandine Bellec** ( amandine.bellec@univ-paris-diderot.fr )
Université de Paris / CNRS https://orcid.org/0000-0001-7410-9736

**Article**

**Keywords:** single spin crossover molecules, spin states

**Posted Date:** March 16th, 2021

**DOI:** https://doi.org/10.21203/rs.3.rs-251042/v1

# Addressing single spin-crossover molecules in a two dimensional monolayer

Yongfeng Tong,[1] Massine Kelaï,[1] Kaushik Bairagi,[1,*] Vincent Repain,[1] Jérôme Lagoute,[1] Yann Girard,[1] Sylvie Rousset,[1] Marie-Laure Boillot,[2] Talal Mallah,[2] Cristian Enachescu,[3] and Amandine Bellec[1,†]

[1] *Université de Paris, Laboratoire Matériaux et Phénomènes Quantiques, CNRS, F-75013, Paris, France*

[2] *Institut de Chimie Moléculaire et des Matériaux d'Orsay, Université Paris-Saclay, CNRS, UMR 8182, 91405 Orsay 12 Cedex, France*

[3] *Faculty of Physics, Alexandru Ioan Cuza University of Iasi, Iasi 700506, Romania*

## Abstract

Bistable spin-crossover molecules are particularly interesting to the development of innovative electronic and spintronic devices as they present two spin states that can be controlled by external stimuli. In this purpose, being able to switch at will the spin state of a single molecule in a dense molecular array is a key milestone. However, the elastic interactions between the molecules favour more cooperative behaviour where patches of neighbouring molecules switches simultaneously. We demonstrate here that the interaction of iron II spin-crossover molecules with a metallic substrate can strongly reduce their cooperative behaviour until addressing independently single molecular spin state. Mechanoelastic model is able to reproduce well such findings.

* present address: Université Grenoble Alpes, CEA, CNRS, Grenoble INP, IRIG-SPINTEC, 38054 Grenoble, France

† amandine.bellec@univ-paris-diderot.fr

Molecular electronics and spintronics aim at using molecules as elementary components [1–3]. In particular, switchable single molecules [4–8] are attracting lot of interest for applications such as memory devices. In this purpose, spin-crossover molecules can be viewed as promising molecules as they present two spin states which can be addressed by external stimuli such as temperature or light [9–11]. Since the discovery of compounds showing a first order thermal transition [12], the possibility to use spin-crossover molecules as memory has been investigated [13–15]. In bulk material, the key parameter to promote abrupt thermal transition is the short and long elastic interactions inducing cooperativity among the molecules [16]. The size decrease, mandatory to incorporate such molecules in electronic devices, completely modifies the cooperativity as demonstrated for nanoparticules [17–19] and thin films [20, 21]. Interestingly, at the molecular scale, the concept of memristance has been demonstrated for isolated single spin-crossover molecules adsorbed on a substrate [22, 23]. This has been made possible because the molecules were decoupled from the metallic layer. Indeed, in direct contact with a metallic substrate, the molecule's spin state is usually locked without possibility to modify it [24].

The idea of addressing single molecules inside a self-assembled layer implies that the cooperativity have to be reduced so that the molecules are essentially independent from each other. Here we focus our study on the interplay between cooperativity and molecule-substrate interaction along with their impact on the bistability of single spin-crossover molecules self-organized in monolayer islands adsorbed on metallic substrates, namely Au(111) and Cu(111). We demonstrate by scanning tunneling microscopy measurements the possibility to address a single molecule inside a self-assembled molecular layer in direct contact with a metal. These experimental results are supported by mechanoelastic simulations that highlight the influence of the molecule-substrate interaction on the correlation between the molecules as well as on the cluster relaxation and consequently on the cooperativity inside the molecular layer.

The two dimensional molecular layers grown on metallic substrates are composed of $[Fe^{II}((3,5\text{-}(CH_3)_2Pz)_3BH)_2]$ (Pz = pyrazolyl) spin-crossover molecules, called FeMPz in the following, which have a hysteretic thermal transition at a temperature around 190 K in bulk [25]. On both Au(111) and Cu(111) substrates, the molecules FeMPz self-assembled in a molecular 2D network (see SI for details) [26, 27]. Figure 1.a presents a typical STM topographic image on Cu(111) of the thermal state which corresponds to the state at low

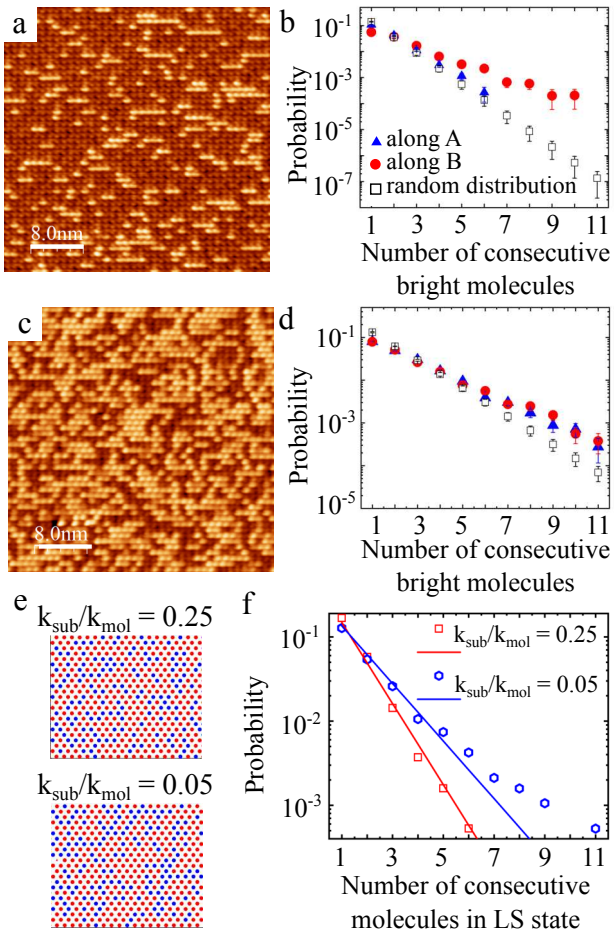


FIG. 1. Cooperativity in the molecular network on Cu(111) for the thermal and photoexcited states. a) $40 \times 40$ nm$^2$ STM topographic image of the thermal state at $V = 0.3$ V and $I = 5$ pA. b) Probability to have $n$ consecutive bright molecules in the thermal state measured along $\vec{A}$ (blue triangles) and $\vec{B}$ (red dots) and compared to a random distribution (empty squares). c) $40 \times 40$ nm$^2$ STM topographic image of the photoexcited state at $V = 0.3$ V and $I = 5$ pA. d) Probability to have $n$ consecutive bright molecules in the photoexcited state measured along $\vec{A}$ (blue triangles) and $\vec{B}$ (red dots) and compared to a random distribution (empty squares). e) Snapshots of the thermal state for $k_{mol} = 4$ N.m$^{-1}$ and $k_{sub} = 1$ N.m$^{-1}$ (top) and $k_{sub} = 0.2$ N.m$^{-1}$ (bottom). The molecules in LS (HS) state are coded in blue (red). f) Probabilities to have $n$ consecutive molecules in LS state in red for $k_{sub} = 1$ N.m$^{-1}$ and in blue for $k_{sub} = 0.2$ N.m$^{-1}$. The probabilities obtained from the mechanoelastic model (symbols) are compared to a random distribution (lines).

temperature after the thermal transition. This state is measured at 4.6 K and at a bias voltage of 0.3 V just after cooling down the sample from room temperature (tip approach and scanning at 0.3 V and 50 pA to avoid any switching of the molecules, see below). The molecules in the network appear either bright or dark which indicates the co-existence of molecules with different electronic properties. The proportion of bright molecules ($p_b$) measured for the thermal state is $0.25 \pm 0.03$ (average over around 12500 molecules counted in five STM images). The comparison with x-ray absorption spectroscopy measurements [28] indicates that the bright molecules at 0.3 V are in the low spin (LS) state while the dark ones are in the high spin (HS) state similarly to what is observed on Au(111) (see Figure S2 in SI). The main difference between the Cu and Au substrates is the organization of the bright molecules at 0.3 V. Indeed, on Au(111) a superstructure is observed over a large area (up to $100 \times 100$ nm$^2$) [26] indicating strong interactions between the molecular spin states. For the Cu(111), the distribution of the bright molecules seems more random (compare Figure 1.a and Figure S2). To have a better understanding of the bright molecule distribution, we measured the probability of observed $n$ consecutive bright molecules along $\vec{A}$ (blue triangles) and along $\vec{B}$ (red points) as reported in Figure 1.b. The measured probabilities are compared to the probability, given by $p_b^n(1-p_b)^2$, to have $n$ consecutive bright molecules for a random distribution of bright molecules. As one can see, the measured probabilities are larger than what is expected for a random distribution especially along the direction $\vec{B}$. This indicates that, when adsorbed on Cu(111), correlations exist between the molecules even though they are weaker than on Au(111).

We investigate the photoexcitation at the molecular scale under blue light. Figure 1.c presents a typical STM topographic image obtained under blue light after saturation, i.e. no more evolution is measured. One can see that more molecules are appearing bright than in the thermal state. The maximum conversion from the high spin state to the low spin state, i.e. from dark to bright molecules at a bias voltage of 0.3 V, leads to an increase of $p_b$ to $0.47 \pm 0.02$ (average over around 12500 molecules counted in five STM images). Once again, this proportion of bright molecules is consistent with the proportion of LS molecules measured by XAS [28]. For the photoexcited state, the probabilities to find $n$ consecutive bright molecules along $\vec{A}$ and $\vec{B}$ are only slightly higher than for a random distribution (Figure 1.d). The photoexcitation, happening randomly, seems to suppress the local correlations. Qualitatively, the photoexcitation on both substrates can be compared.

For the Au(111) substrate, internal dynamics was observed during the photoexcitation which we suspected to come from elastic interactions inside the molecular layer [26]. In contrast, on the Cu(111) substrate, the STM images seem less noisy with an increase of the bright molecule number and very few reverse transition (from bright to dark) as can be seen in the film in SI. This qualitative comparison once again underlines the fact that the interaction between the molecules are modified depending on the metallic substrate used and that the correlations are far larger in the molecular film grown on Au(111) than on Cu(111).

Using mechanoelastic simulations [29–31], we investigate the influence of the molecule-susbtrate interaction on the local correlations. In this purpose, we fixed a value for the intermolecular interaction ($k_{mol}$) to 4 N.m$^{-1}$ and calculated the thermal state for two different molecule-substrate interactions ($k_{sub}$ = 0.2 and 1 N.m$^{-1}$), which are represented in Figure 1.e. The first consequence of the $k_{sub}$ variation is the proportion in the thermal state of molecules in low and high spin states, as previously reported [27]. We obtained proportions of molecules in low spin state ($p_{LS}$) of 0.46 and 0.34 for $k_{sub}$ values of 0.2 and 1 N.m$^{-1}$, respectively. As presented in Figure 1.f, we then determined in the thermal state the probability to have $n$ consecutive molecules in low spin state along the three equivalent directions of the triangular lattice. It appears that for a $k_{sub}$ value of 1 N.m$^{-1}$ the probability to have $n$ consecutive molecules in low spin state follows a random distribution (lines in Figure 1.f). On the contrary, for a reduced value of $k_{sub}$ (0.2 N.m$^{-1}$), the measured probability is away from the random distribution. Correlation between the molecules can also be quantified through the Moran index which decreases while the interaction to the substrate increases (see Figure S3 in SI). Thus, increasing the interaction between the molecules and the substrate leads to the decrease of the correlations inside the molecular layer. Once again this suggests that the molecules interact more with the Cu(111) substrate than with the Au(111).

Voltage pulses can also be used to trigger the transition of a single molecule from one spin state to the other [22, 23, 32]. The manipulation with voltage pulses has thus been tested on both metallic substrates. Figure 2.a and 2.b presents two examples of voltage pulses applied on molecules adsorbed on Au(111). For the first example, a series of four consecutive pulses of 0.6 V (for 10 ms) is applied on four nearby molecules - two bright and two dark at 0.3 V as schematized by the black points in Figure 2.a. Interestingly, as can be seen in the STM topographic image recorded after the voltage pulse application, the

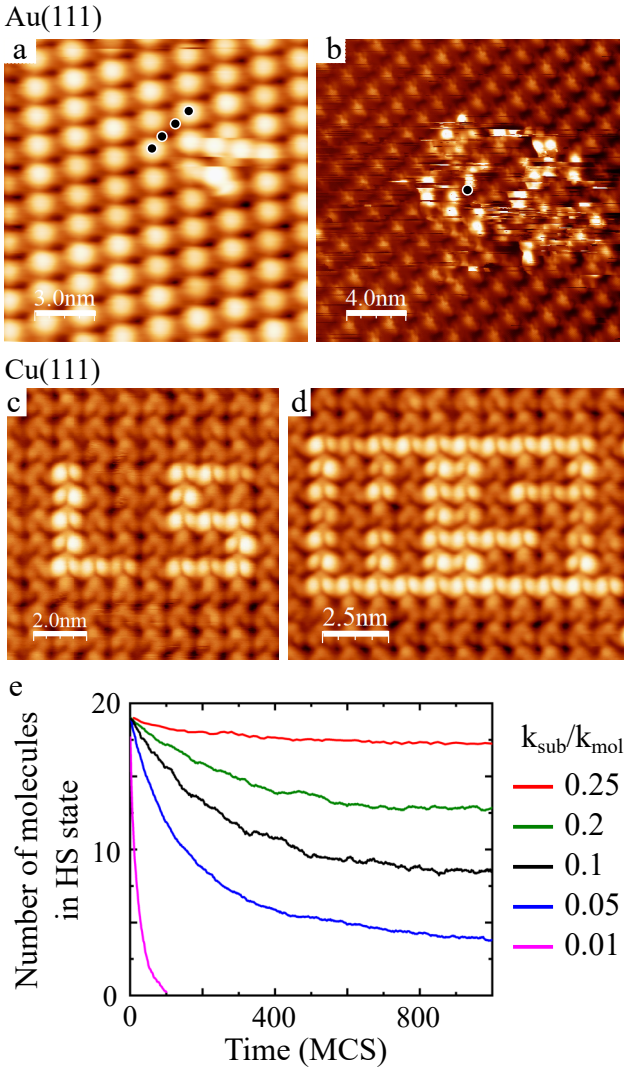


FIG. 2. Induced switching by voltage pulses. a) 15×15 nm$^2$ STM topographic image acquired after the application of four voltage pulses at 0.6 V on the different application points marked by the black dots ($V = 0.3$ V, $I = 20$ pA, z varies from 0 to 1.7 Å). b) 20×20 nm$^2$ STM current image after a voltage pulse at 2.2 V (10 ms) applied at the location of the black dot ($V = 0.3$ V, $< I >= 10$ pA, I varies from 0 to 250 pA). c) $10 \times 10$ nm$^2$ and d) $10 \times 12.5$ nm$^2$ topographic images where "LS" and "HS" have been written by voltage pulses ($V = 0.3$ V, $I = 3$ pA, z varies from 0 to 2.63 Å). e) Relaxation of a cluster of molecules in HS state in an environment of molecules in LS state as a function of time (in Monte Carlo steps) for different ratio of $k_{sub}/k_{mol}$ with $k_{mol} = 4$ N.m$^{-1}$.

molecules on which the pulses have been applied are still in their initial state while a defect of bright molecules has appeared nearby, evidencing a non-local switching process [32]. The

4-bright-molecule defect is stabilized for a few minutes (typically two minutes) before the network recovers its initial superstructure (see Figure S4 in SI). Applying larger voltage pulse can lead to the formation of larger defective area as presented in Figure S4 (see SI), where lines of four or seven bright molecules are observed. Most probably, these 4-bright-molecule and 7-bright-molecule lines can be stabilized because of their commensurability with the thermal state superstructure [26]. Another example of voltage pulse is given in Figure 2.b. The voltage pulse of 2.2 V applied in the middle of the image induces the local creation of a phase-shifted domain. As visible in Figure S5, the inner domain shrinks within a few scans (less than fifteen minutes). Once again the created defect, here a phase-shifted domain, is quickly healed. All these examples clearly show that applying voltage pulses enables the conversion of some molecules from the HS state to the LS one (dark to bright) but the elastic interactions within the 2D network (cooperativity) prevents addressing a single molecule and keeping the created defects or phase-shifted domains on Au(111).

On the contrary, on Cu(111), we demonstrated the possibility to address the molecules one by one in the 2D network. Figures 2.c and 2.d present STM images where first the molecules have been switched to the dark state, then one by one some molecules have been switched back to the bright state to write HS and LS (the switching procedure is discussed below). These features have been scanned for thirteen hours at a bias voltage of 0.3 V and as can be seen in Figure S6 they remain intact with only few visible defects.

To explain the role of the substrate on the stability of the switched molecules, we performed a second mechanoelastic simulation. The initial state consists in a cluster of nineteen molecules in the HS state surrounded by molecules in LS state. The relaxation of the HS molecules in the cluster is simulated for different $k_{sub}/k_{mol}$ ratios for a given $k_{mol}$ of 4 N.m$^{-1}$. The relaxation curves in Figure 2.e are obtained by averaging 100 relaxation curves (see Figure S7 in SI). The typical relaxation time for the cluster increases as the value of $k_{sub}$ increases. This indicates that the spin state of the molecules can be stabilized by the substrate interaction. This is in very good agreement with our observation that a switched state is more stable on Cu(111) than on Au(111).

We then investigated in more details the tunneling conditions to switch the molecules from one spin state to the other on Cu(111). The first observation was realized by scanning a photoexcited area at 0.7 V. We observed by zooming out that in the area scanned at 0.7 V all the molecules are now appearing black at 0.3 V with clear-cut edges (see Fig. S8

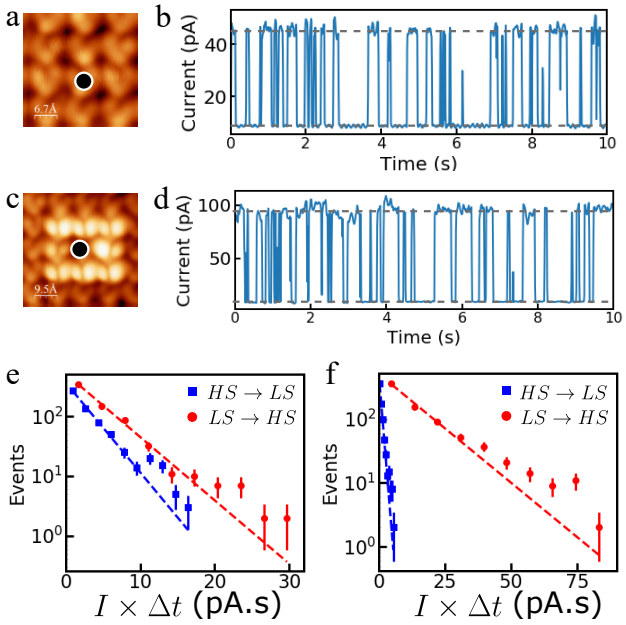


FIG. 3. Voltage pulses on Cu(111). a) $3.5 \times 3.5$ nm$^2$ STM topographic image of the initial state with dark (HS) neighbours ($V = 0.3$ V, $I = 5$ pA) and c) $4.8 \times 4.8$ nm$^2$ STM topographic image of the initial state with bright (LS) neighbours ($V = 0.3$ V, $I = 5$ pA). The black dots indicate the position of the voltage pulses in both environments. b), d) Typical $I(t)$-traces recorded during voltage pulses of 0.5 V for dark (HS) and bright (LS) neighbours, respectively. e), f) Distribution of current times duration ($I \times \Delta t$) of each plateau of the $I(t)$-traces for dark (HS) and bright (LS) neighbours, respectively. The red circles (blue squares) correspond to the experimental distribution of events from bright (LS) to dark (HS) (dark (HS) to bright (LS)) molecules. The dotted lines correspond to mono-exponential fits of each distribution.

in SI). Thus, for this voltage bias the molecular switching from the LS state to the HS state is favoured. The reverse switching can also be induced by using lower bias values. To investigate in more details the possibility to locally induce the switching of the molecules at positive voltage along with the influence of their first neighbours, we considered two initial situations: either a molecule surrounded by dark (HS) molecules (Figure 3.a) or a molecule surrounded by bright (LS) molecules (Figure 3.c). For both cases, it exists a threshold voltage of 0.45 V below which no switching is observed within the temporal window of a few minutes. Above this threshold, the switching can be induced. During voltage pulses of 0.5 V, the tunneling current has been recorded as a function of time and typical $I(t)$-traces

are presented in Figures 3.b and 3.d for dark (HS) or bright (LS) neighbours, respectively. From the analysis of the $I(t)$-traces, it is possible to extract a yield for the switching from the HS state (dark) to the LS state (bright) ($Y_{HS\rightarrow LS}$) and from the LS state (bright) to the HS state (dark) ($Y_{LS\rightarrow HS}$) for both environments. The yield is defined as $Y = \frac{e}{I\tau}$, with $e$ the electron charge, $I$ and $\tau$ the characteristic current and time for each switching extracted from the distribution of the current times duration (see Figures 3.e and 3.f and SI ). When surrounded by molecules in the HS state, both switching events (from HS to LS and LS to HS) are equally probable with equivalent yield values of $Y_{HS\rightarrow LS} = 5.5\ 10^{-8}$ and $Y_{LS\rightarrow HS} = 3.9\ 10^{-8}$. On the contrary, when surrounded by molecules in the LS state, the switching yield from HS-to-LS ($Y_{HS\rightarrow LS} = 18.6\ 10^{-8}$) is one order of magnitude larger than the switching yield from LS-to-HS ($Y_{LS\rightarrow HS} = 1.3\ 10^{-8}$). Often, the final state imaged after the voltage pulse reveals that some of the bright neighbours are switched to the dark state. Nonetheless, this clearly underlines that if the molecules can be addressed individually, the neighbourhood is still influencing the switching properties. For higher bias voltage values, the current traces are more noisy and the HS state is favoured as evidenced by the possibility to create 'dark' area. Thus, on Cu(111) substrate, molecules can be individually addressed thanks to the molecule-substrate interaction. The cooperativity is only reduced as evidenced by the modification of the switching properties of a given molecule by its first neighbour's spin state.

The different experiments and simulations described here highlight the role of the substrate nature on the local correlation in the molecular layers and the possibility to stabilize at will a molecule in a given spin state. The molecular layer on Au(111) presents a strong cooperativity as evidenced by the long range correlation in the superstructure and the impossibility to control or stabilize any specific feature. On Cu(111), the stronger molecule-substrate interaction weakens the cooperativity in the molecular layer, thus enabling to address and stabilize the spin state of single molecules. The possibility to address single molecule in a dense and organized network is interesting for future memory devices at the molecular scale.

## METHODS

### Experimental methods

Prior to the molecular deposition, the metallic Cu(111) and Au(111) single crystals are cleaned under ultra high vacuum (UHV, base pressure of $10^{-10}$ mbar) by sputtering ($Ar^+$ ions at 600 eV or 900 eV for Cu(111) or Au(111) respectively) and annealing (450° C for both substrates) cycles. Molecules FeMPz are then sublimated under UHV at a temperature of 85°C from a home-made Knudsen-cell-like evaporator on the metallic substrate. During the molecular sublimation the single crystals are kept at low temperature (around 5 K). The samples are then annealed at room temperature to enable the formation of the molecular islands. All the measurements have been carried out on a low temperature scanning tunneling microscope (STM, Omicron) operating at 4.6 K. The light excitation has been realized thanks to a super-continuum white laser followed by a filter (SuperK Evo/Varia, NKTPhotonics) working at $405 \pm 5$ nm with a power of 1.5 mW at the end of the optical fibre before the UHV chamber.

### Mechanoelastic simulations

For the mechanoelastic simulations, spin-crossover molecules are represented as balls arranged in a triangular configuration and linked to their first neighbours situated in the same layer by springs with an elastic constant $k_{mol}$. The ball radii code for the molecular spin states by taking a value of 0.22 nm and 0.2 nm for the HS and the LS states, respectively. The distance between two LS molecule centres is 1 nm. The interaction to the substrate is taken into account by linking each spin-crossover molecule to three surface molecules in a face centred cubic configuration by springs with an elastic constant $k_{sub}$. The intrinsic parameters of the system are $\Delta H = 1500 \times 10^{-23}$ J and $\Delta S = 9.7 \times 10^{-23}$ $J.K^{-1}$, thus giving a thermal transition temperature around 155 K.

## ACKNOWLEDGMENTS

The authors thank the European Union's Horizon 2020 research and innovation program under grant agreement n° 766726 for support. C.E. thanks UEFISCDI Romania (grant

number PN-III-P4-ID-PCE-2020-1946).

[1] M. Cinchetti, V. A. Dediu, and L. E. Hueso, Nature Materials **16**, 507 (2017).

[2] S. Delprat, M. Galbiati, S. Tatay, B. Quinard, C. Barraud, F. Petroff, P. Seneor, and R. Mattana, Journal of Physics D: Applied Physics **51**, 473001 (2018).

[3] E. Coronado, Nature Reviews Materials **5**, 87 (2019).

[4] H. Böckmann, S. Liu, J. Mielke, S. Gawinkowski, J. Waluk, L. Grill, M. Wolf, and T. Kumagai, Nano Letters **16**, 1034 (2016).

[5] C. Nacci, M. Baroncini, A. Credi, and L. Grill, Angewandte Chemie International Edition **57**, 15034 (2018).

[6] A. Köbke, F. Gutzeit, F. Röhricht, A. Schlimm, J. Grunwald, F. Tuczek, M. Studniarek, D. Longo, F. Choueikani, E. Otero, P. Ohresser, S. Rohlf, S. Johannsen, F. Diekmann, K. Rossnagel, A. Weismann, T. Jasper-Toennies, C. Näther, R. Herges, R. Berndt, and M. Gruber, Nature Nanotechnology **15**, 18 (2020).

[7] R. Harsh, F. Joucken, C. Chacon, V. Repain, Y. Girard, A. Bellec, S. Rousset, R. Sporken, A. Smogunov, Y. J. Dappe, and J. Lagoute, The Journal of Physical Chemistry Letters **10**, 6897 (2019).

[8] M. Bouatou, C. Chacon, F. Joucken, Y. Girard, V. Repain, A. Bellec, S. Rousset, R. Sporken, C. González, Y. J. Dappe, and J. Lagoute, The Journal of Physical Chemistry C **124**, 15639 (2020).

[9] J. A. Real, A. B. Gaspar, and M. C. Muñoz, Dalton Transactions , 2062 (2005).

[10] W. Nicolazzi and A. Bousseksou, Comptes Rendus Chimie **21**, 1060 (2018).

[11] J. Dugay, M. Aarts, M. Gimz-Marqu T. Kozlova, H. W. Zandbergen, E. Coronado, and H. S. J. van der Zant, Nano Letters **17**, 186 (2017).

[12] W. A. Baker and H. M. Bobonich, Inorganic Chemistry **3**, 1184 (1964).

[13] O. Kahn and J. Launay, Chemtronics **3**, 140 (1988).

[14] O. Kahn, J. Kröber, and C. Jay, Advanced Materials **4**, 718 (1992).

[15] O. Kahn and C. J. Martinez, Science **279**, 44 (1998).

[16] K. Ridier, G. Molnár, L. Salmon, W. Nicolazzi, and A. Bousseksou, Solid State Sciences **74**, A1 (2017).

[17] F. Volatron, L. Catala, E. Rivière, A. Gloter, O. Stéphan, and T. Mallah, Inorganic Chemistry **47**, 6584 (2008).

[18] G. Félix, W. Nicolazzi, L. Salmon, G. Molnár, M. Perrier, G. Maurin, J. Larionova, J. Long, Y. Guari, and A. Bousseksou, Physical Review Letters **110** (2013).

[19] R. Bertoni, M. Lorenc, H. Cailleau, A. Tissot, J. Laisney, M.-L. Boillot, L. Stoleriu, A. Stancu, C. Enachescu, and E. Collet, Nature Materials **16**, 606 (2016).

[20] T. Groizard, N. Papior, B. Le Guennic, V. Robert, and M. Kepenekian, The Journal of Physical Chemistry Letters **8**, 3415 (2017).

[21] L. Kipgen, M. Bernien, S. Ossinger, F. Nickel, A. J. Britton, L. M. Arruda, H. Naggert, C. Luo, C. Lotze, H. Ryll, F. Radu, E. Schierle, E. Weschke, F. Tuczek, and W. Kuch, Nature Communications **9**, 2984 (2018).

[22] T. Miyamachi, M. Gruber, V. Davesne, M. Bowen, S. Boukari, L. Joly, F. Scheurer, G. Rogez, T. K. Yamada, P. Ohresser, E. Beaurepaire, and W. Wulfhekel, Nature Communications **3**, 938 (2012).

[23] T. Jasper-Tönnies, M. Gruber, S. Karan, H. Jacob, F. Tuczek, and R. Berndt, Nano Letters **17**, 6613 (2017).

[24] M. Gruber, V. Davesne, M. Bowen, S. Boukari, E. Beaurepaire, W. Wulfhekel, and T. Miyamachi, Physical Review B **89**, 195415 (2014).

[25] O. Iasco, M.-L. Boillot, A. Bellec, R. Guillot, E. Rivière, S. Mazerat, S. Nowak, D. Morineau, A. Brosseau, F. Miserque, V. Repain, and T. Mallah, Journal of Materials Chemistry C **5**, 11067 (2017).

[26] K. Bairagi, O. Iasco, A. Bellec, A. Kartsev, D. Li, J. Lagoute, C. Chacon, Y. Girard, S. Rousset, F. Miserque, Y. J. Dappe, A. Smogunov, C. Barreteau, M.-L. Boillot, T. Mallah, and V. Repain, Nature Communications **7**, 12212 (2016).

[27] C. Fourmental, S. Mondal, R. Banerjee, A. Bellec, Y. Garreau, A. Coati, C. Chacon, Y. Girard, J. Lagoute, S. Rousset, M.-L. Boillot, T. Mallah, C. Enachescu, C. Barreteau, Y. J. Dappe, A. Smogunov, S. Narasimhan, and V. Repain, The Journal of Physical Chemistry Letters **10**, 4103 (2019).

[28] L. Zhang, Y. Tong, M. Kelai, A. Bellec, J. Lagoute, C. Chacon, Y. Girard, S. Rousset, M.-L. Boillot, E. Rivière, T. Mallah, E. Otero, M.-A. Arrio, P. Sainctavit, and V. Repain, Angewandte Chemie International Edition **59**, 13341 (2020).

[29] C. Enachescu, L. Stoleriu, A. Stancu, and A. Hauser, Physical Review Letters **102**, 257204 (2009), publisher: American Physical Society.

[30] C. Enachescu, M. Nishino, S. Miyashita, L. Stoleriu, and A. Stancu, Physical Review B **86**, 054114 (2012).

[31] C. Enachescu and A. Hauser, Physical Chemistry Chemical Physics **18**, 20591 (2016).

[32] T. G. Gopakumar, F. Matino, H. Naggert, A. Bannwarth, F. Tuczek, and R. Berndt, Angewandte Chemie International Edition **51**, 6262 (2012).

# Figures

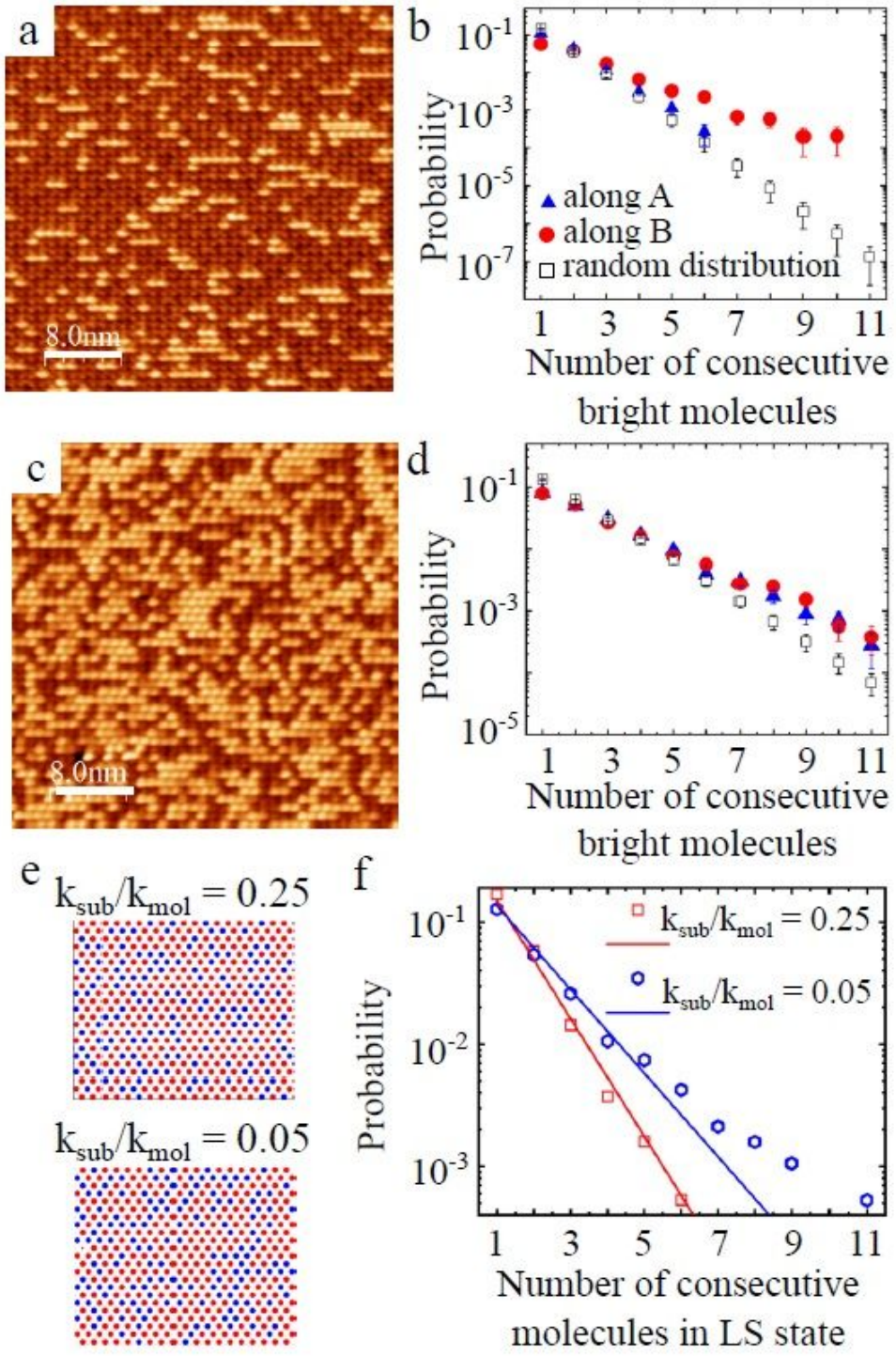


**Figure 1**

Cooperativity in the molecular network on Cu(111) for the thermal and photoexcited states. a) 40 x 40 nm2 STM topographic image of the thermal state at V = 0:3 V and I = 5 pA. b) Probability to have n consecutive bright molecules in the thermal state measured along ~A (blue triangles) and ~B (red dots)

and compared to a random distribution (empty squares). c) 40 x 40 nm2 STM topographic image of the photoexcited state at V = 0:3 V and I = 5 pA. d) Probability to have n consecutive bright molecules in the photoexcited state measured along ~A (blue triangles) and ~B (red dots) and compared to a random distribution (empty squares). e) Snapshots of the thermal state for kmol = 4 N.m-1 and ksub = 1 N.m-1 (top) and ksub = 0.2 N.m-1 (bottom). The molecules in LS (HS) state are coded in blue (red). f) Probabilities to have n consecutive molecules in LS state in red for ksub = 1 N.m-1 and in blue for ksub = 0.2 N.m-1. The probabilities obtained from the mechanoelastic model (symbols) are compared to a random distribution (lines).

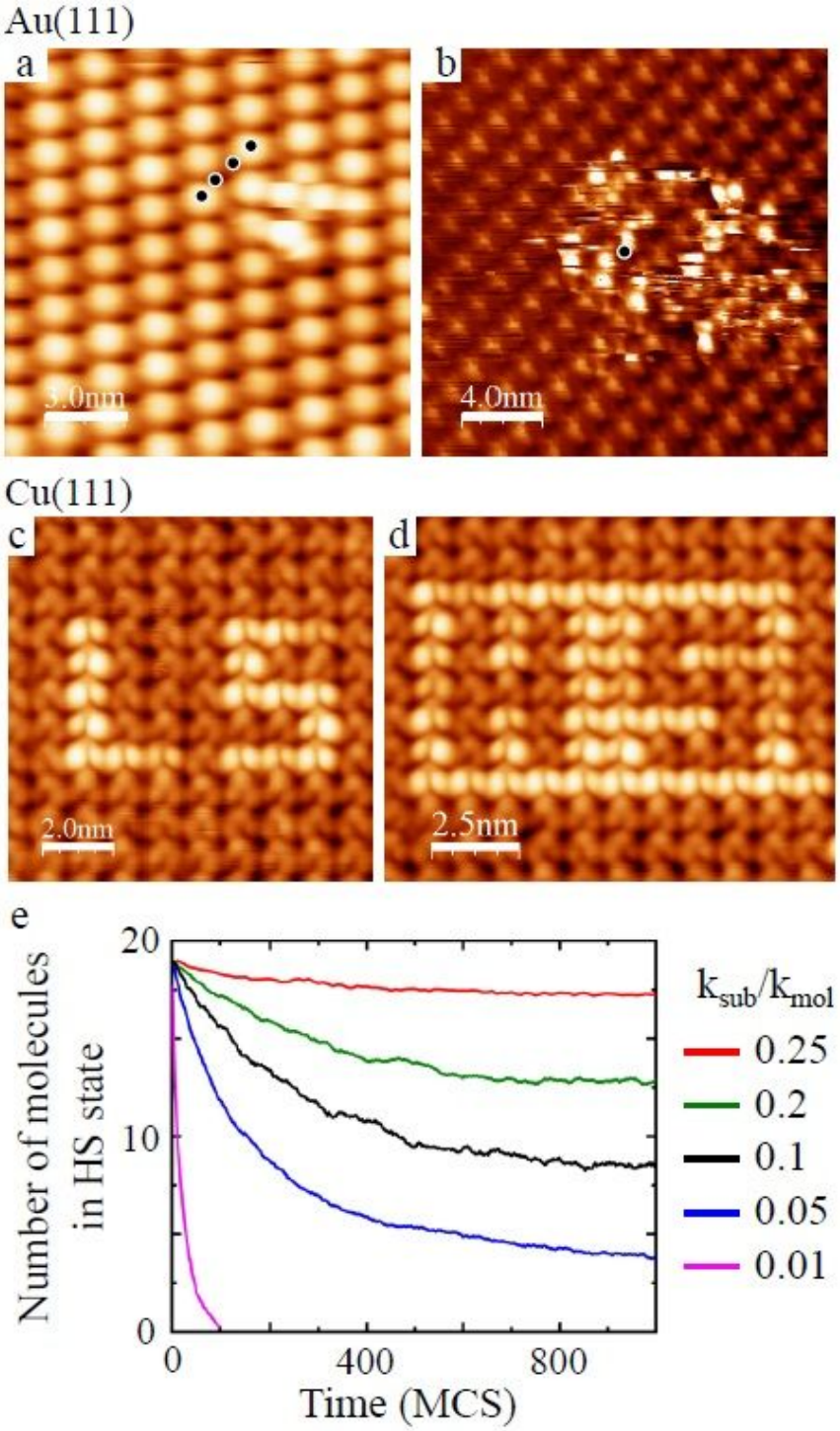


**Figure 2**

Induced switching by voltage pulses. a) 15 x 15 nm2 STM topographic image acquired after the application of four voltage pulses at 0.6 V on the different application points marked by the black dots (V = 0:3 V, I = 20 pA, z varies from 0 to 1.7 A). b) 20 x 20 nm2 STM current image after a voltage pulse at 2.2 V (10 ms) applied at the location of the black dot (V = 0:3 V, < I >= 10 pA, I varies from 0 to 250 pA). c) 10 x 10 nm2 and d) 10 12:5 nm2 topographic images where \LS" and \HS" have been written by voltage

pulses (V = 0:3 V, I = 3 pA, z varies from 0 to 2.63 A). e) Relaxation of a cluster of molecules in HS state in an environment of molecules in LS state as a function of time (in Monte Carlo steps) for different ratio of ksub=kmol with kmol = 4 N.m-1.

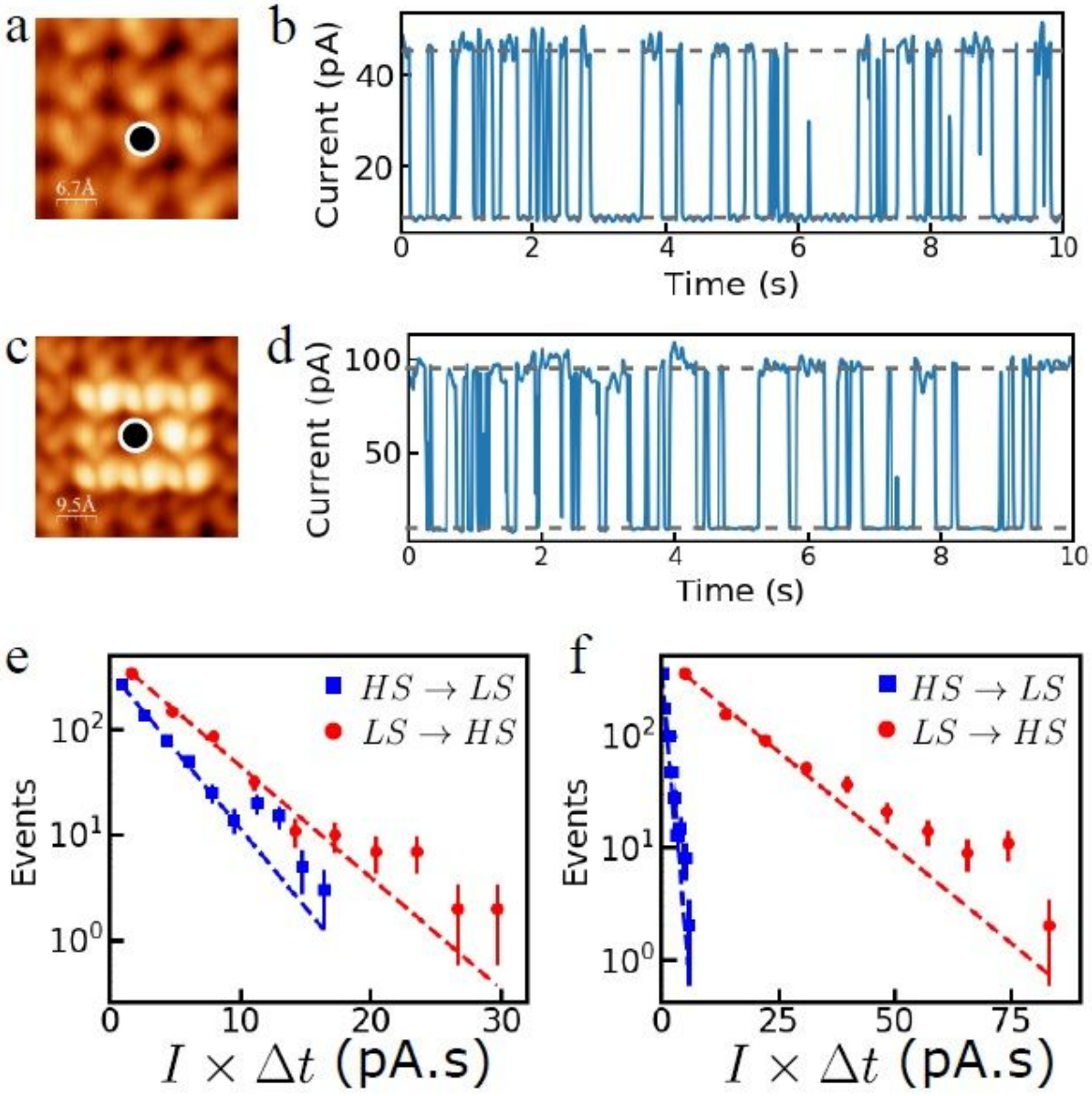


**Figure 3**

Voltage pulses on Cu(111). a) 3:5 x 3:5 nm2 STM topographic image of the initial state with dark (HS) neighbours (V = 0:3 V, I = 5 pA) and c) 4:8 x 4:8 nm2 STM topographic image of the initial state with bright (LS) neighbours (V = 0:3 V, I = 5 pA). The black dots indicate the position of the voltage pulses in both environments. b), d) Typical I(t)-traces recorded during voltage pulses of 0.5 V for dark (HS) and bright (LS) neighbours, respectively. e), f) Distribution of current times duration (It) of each plateau of the

I(t)-traces for dark (HS) and bright (LS) neighbours, respectively. The red circles (blue squares) correspond to the experimental distribution of events from bright (LS) to dark (HS) (dark (HS) to bright (LS)) molecules. The dotted lines correspond to mono-exponential ts of each distribution.

## Supplementary Files

This is a list of supplementary files associated with this preprint. Click to download.

- Tongetalfilm.mp4
- TongetalSI.pdf